ARTICLE - Acute Lymphoblastic Leukemia

Interleukin signaling mitigates the inhibitory effects of combined Src/BCR-ABL1 blockade on T-cell activity in Philadelphia chromosome-positive acute lymphoblastic leukemia

Farnaz Naeemikia,[1] Joshua Reynolds,[1] Cheng Dong[1] and Justin R Pritchard[1,2]

[1]Department of Biomedical Engineering and [2]Huck Institute for the Life Sciences, University Park, The Pennsylvania State University, PA, USA

Correspondence: J.R. Pritchard
Jrp94@psu.edu

Received: August 4, 2025.
Accepted: January 16, 2026.
Early view: February 5, 2026.

https://doi.org/10.3324/haematol.2025.288829

Supplemental Experimental Methods:

Cell Lines and Primary Cells

The human acute T-cell leukemia cell line Jurkat, Clone E6-1 (ATCC, Cat. No. TIB-152), Jurkat-IL-2-Luciferase, Jurkat-NFAT-Luciferase, and the Philadelphia chromosome-positive (Ph+) pre-B leukemia cell line BV173 (DSMZ, Cat. No. ACC 20) were utilized for this study. All cell lines were maintained in RPMI 1640 Medium (Gibco, Cat. No. 11875093) supplemented with 10% heat-inactivated Fetal Bovine Serum (FBS) (Gibco, Cat. No. 26140079) and 1% Penicillin-Streptomycin (Gibco, Cat. No. 15140122). Cultures were maintained in a humidified incubator at 37°C with 5% CO_2.

Primary human T cells were obtained from peripheral blood mononuclear cells (PBMCs) of two healthy donors purchased from STEMCELL Technologies. T cells were isolated and expanded to >90% purity using the ImmunoCult™ Human CD3/CD28 T Cell Activator kit (STEMCELL Technologies, Cat. No. 10971). For specific T-cell stimulation assays, Dynabeads™ Human T-Activator CD3/CD28 (Thermo Fisher Scientific, Cat. No. 11131D) were used.

Reagents and Therapeutics

Tyrosine Kinase Inhibitors (TKIs): Ponatinib, dasatinib, nilotinib, and imatinib were used. Stock solutions (10–20 mM) were prepared in 100% DMSO and stored at −20°C. Working concentrations were freshly diluted, ensuring the final DMSO concentration in cultures did not exceed 0.1% (v/v).

Clinically relevant concentrations (CRC): ponatinib (30 nM), dasatinib (10 nM), nilotinib (130 nM), imatinib (450 nM)[1];

Peak plasma concentrations (Cmax): ponatinib (145 nM), dasatinib (150 nM), nilotinib (3000 nM), imatinib (3000 nM)[1].

Bispecific T-Cell Engager (BiTE): Blinatumomab (Blincyto®, Amgen) was reconstituted according to supplier instructions and used at a working concentration of 1 ng/mL unless otherwise specified.

Recombinant Interleukins: Recombinant human IL-2 (PeproTech, Cat. No. 200-02), IL-7 (PeproTech, Cat. No. 200-07), and IL-15 (PeproTech, Cat. No. 200-15) were reconstituted per the manufacturer's instructions and stored as aliquots at −20°C. A working concentration of 10 ng/mL was used for all rescue experiments.

T-Cell Stimulation and Signaling Analysis

For LCK phosphorylation analysis, Jurkat T cells were serum-starved overnight. Cells were then pre-treated with TKIs or a vehicle control (0.1% DMSO) for 2-4 hours, followed by stimulation with Dynabeads™ CD3/CD28 or soluble anti-CD3/CD28 antibodies for time points ranging from 10 minutes to 4 hours.

For STAT5 signaling analysis, Jurkat or primary T cells were first stimulated with recombinant interleukins (10 ng/mL) for 4 hours, followed by TKI treatment and a brief 10-minute stimulation with CD3/CD28 Dynabeads before lysis.

Western Blotting

Following stimulation, cells were harvested and lysed on ice using PhosphoSafe™ Extraction Reagent (Millipore Sigma, Cat. No. 71296-3). Total protein concentration was quantified using the Pierce™ BCA Protein Assay Kit (Thermo Fisher, Cat. No. 23225). Equal amounts of protein (10-20 µg) were loaded onto 4-12% NuPAGE™ Bis-Tris precast gels (Invitrogen) and resolved by SDS-PAGE using NuPAGE™ MOPS SDS Running Buffer. Proteins were transferred to a nitrocellulose membrane using NuPAGE™ Transfer Buffer. Membranes were blocked for 1 hour with 5% Bovine Serum Albumin (BSA) in TBST and incubated overnight at 4°C with the following primary antibodies:

anti-phospho-LCK (Y394) (R&D Systems, Cat. No. MAB8138), anti-total LCK (Cell Signaling Technology, Cat. No. 2785), anti-phospho-STAT5 (Y694) (Cell Signaling Technology, Cat. No. 9359), anti-total STAT5 (Cell Signaling Technology, Cat. No. 94205), and anti-GAPDH (Cell Signaling Technology, Cat. No. 5174). Membranes were then incubated with HRP-conjugated secondary antibodies (Cell Signaling Technology), and protein bands were visualized using SuperSignal™ West Pico PLUS Chemiluminescent Substrate (Thermo Fisher, Cat. No. 34580).

Flow Cytometry

For intracellular analysis of LCK phosphorylation, stimulated Jurkat cells were fixed with 4% paraformaldehyde (BioLegend, Cat. No. 420801) and then permeabilized using TruPhosPho™ Perm Buffer (BioLegend, Cat. No. 425801). Cells were subsequently stained with PE anti-human phospho-LCK (Y394) antibody (BioLegend, Cat. No. 651203).

For co-culture assays, cells were harvested and stained with a surface antibody cocktail to identify and quantify distinct cell populations. The panel included the following antibodies, all from BioLegend: FITC anti-human CD4 (Clone RPA-T4, Cat. No. 300506), PE anti-human CD8 (Clone RPA-T8, Cat. No. 301008), APC anti-human CD19 (Clone HIB19, Cat. No. 302212), and PE/Cy7 anti-human PD-1 (Clone EH12.2H7, Cat. No. 329918). Cell viability was assessed using the Zombie NIR™ Fixable Viability Kit (BioLegend, Cat. No. 423105). To determine absolute cell counts, Precision Count Beads™ (BioLegend, Cat. No. 424902) were added to each sample prior to acquisition.

All data were acquired on a BD LSRFortessa™ cell analyzer and were analyzed using FlowJo™ software.

Functional T-Cell Assays

Luciferase Reporter Assays: Jurkat-IL-2-Luciferase or Jurkat-NFAT-Luciferase reporter cells were pre-treated with TKIs for 2-4 hours before being co-cultured with BV173 target cells (E:T ratio 1:1) and blinatumomab (1 ng/mL) for 16 hours. Luciferase activity was measured using the Luciferase Assay System (Promega, Cat. No. E1500) on a multimode plate reader EnVision™. Combination Therapy and Cytotoxicity Assays: Primary human T cells were co-cultured with BV173 target cells (E:T ratio 1:2) for 48-72 hours in the presence of blinatumomab, TKIs, and/or interleukins. For rescue experiments, T cells were pre-incubated overnight with interleukins prior to co-culture. Target cell killing and T-cell proliferation were assessed by flow cytometry.

Supplemental Modeling Methods

Bliss Score

To quantify pharmacologic interaction, we applied the Bliss independence model[2]. Fractional killing for each single agent (Ponatinib and Blinatumomab) was used to calculate the expected additive effect using:

$$E_{A+B} = E_A + E_B - (E_A \cdot E_B)$$

The Bliss score was defined as the difference between the observed combination effect and the predicted Bliss value, with negative values indicating antagonism.

Parameter Estimation and Model Fitting

Parameters for both Model 1 and Model 2 were estimated by fitting the model equations to the experimental time-course data. This was accomplished using a Bayesian framework with Markov Chain Monte Carlo (MCMC) algorithms implemented in MATLAB.

Bayesian Framework and Likelihood Function

The log-likelihood function, which quantifies the probability of observing the experimental data given a specific set of model parameters, was custom-defined assuming a Poisson-distributed measurement error for the cell counts.

Prior Distributions

For each parameter to be estimated, non-informative or weakly informative prior distributions were defined based on existing literature and biological plausibility. This approach constrains the parameter space to reasonable bounds, a critical step in Bayesian inference.

MCMC Methodology:

The log-likelihood function, which quantifies the probability of observing experimental data given a set of parameter values, was custom-defined assuming a Poisson distribution for the measurement error of the cell counts. For each model, 3 independent MCMC chains were initiated. Each chain was run for a total of 10^6 to 10^7 iterations[3,4]. The initial 20-30% of iterations from each chain were discarded as burn-in (based on the parameter that convergence took longer). The post-burn-in chains were thinned by selecting every 100th iteration to reduce autocorrelation, resulting in posterior samples for each parameter.

Convergence Diagnostics:

Trace plots: Visual inspection for mixing and stationarity (Figure S3C-S4A).

Gelman-Rubin statistic ($\hat{R}$): All parameters had $\hat{R} < 1.1$, indicating convergence.

Effective sample size (ESS): All ESS > 1000 (indicative of adequate sampling).

Model Fit Evaluation: The goodness-of-fit of each calibrated model to the experimental data was evaluated both visually and quantitatively. Visual assessment involved overlaying the model simulation (mean of the posterior parameter estimates) against the experimental time-course data (mean ± SEM) (Figure 3A - Figure S3B).

Quantitative metrics used to assess model fit and compare model performance included:

Log-Likelihood (LL): The log-likelihood value calculated at the mean posterior parameter estimates. The log-likelihood quantifies the probability of observing the experimental data given the model and a specific set of parameters. Higher LL values indicate a better fit.

Akaike Information Criterion (AIC): Calculated as $AIC = 2k - 2\ln(LL)$, where k is the number of estimated parameters and LL is the log-likelihood. AIC estimates the relative amount of information lost by a given model and provides a measure of model fit that penalizes for the number of parameters. Lower AIC values indicate a better balance between goodness-of-fit and model complexity.

Bayesian Information Criterion (BIC): Calculated as $BIC = k\ln(n_{obs}) - 2\ln(LL)$, where k is the number of estimated parameters, nobs is the total number of observations used for fitting, and LL is the log-likelihood. Similar to AIC, BIC penalizes for the number of parameters, but applies to a stronger penalty than AIC, particularly for larger datasets. Lower BIC values indicate a preferred model.

For both AIC and BIC, lower values indicate a more parsimonious model that provides a better balance between goodness-of-fit and complexity. The final values for these metrics used for model comparison are provided in Table S1

Table S1: Model Evaluation

Model	k_{free}	n_{obs}	Log Likelihood Mean	AIC	BIC
Model 1	5	84	-9975.1	19960.3	19972.5
Model 2	9	126	-16264.5	2547.08	3257.6

The final parameter estimates for Model 1 (Table S2) and Model 2 (Table S3) were determined by fitting the models to the experimental data.

T-B Model: Basic T–B cell interaction [5–7]**:**

$$\frac{dB}{dt} = r_B\, B\left(1 - \frac{B}{K_B}\right) - a\left(\frac{B^{n_B}}{B^{n_B} + {h_B}^{n_B}}\right)T$$

$$\frac{dT}{dt} = p_T\left(\frac{B^{n_T}}{B^{n_T} + {h_T}^{n_T}}\right)T - d_T\, T$$

Table S2: T-B parameter estimates

T-B Model	Meaning	Units	Priors	Final Estimation
$\mathbf{r_B}$	B cell growth rate	Day^{-1}	fixed	0.63
K	B cell carrying capacity	Cells/ml	fixed	$0.24*10^6$
a	Max killing rate of B cells by T cells	rate × $cells^{-1}$	[0.5,6]	1.6
nB	Hill coefficient for T-mediated killing of B cells	dimensionless	fixed	1
hB	Half-saturation for B cell killing	Cells/ml	[0.01-0.2] $*10^6$	$0.062*10^6$

nT	Hill coefficient for T cell proliferation	dimensionless	fixed	1
h_T	Half-saturation for B-driven T cell proliferation	cells	[0.0001-0.009] *10^6	0.007*10^6
p_T	T cell proliferation rate	Day $^{-1}$	[0.1-3]	1.98
dT	T cell death rate	Day $^{-1}$	[0.001-1.5]	1.2

T-B-Tex Model [8]:

$$\frac{dB}{dt} = r_B\, B\left(1 - \frac{B}{K}\right) - a\left(\frac{B^{n_B}}{B^{n_B} + {h_B}^{n_B}}\right)T$$

$$\frac{dT}{dt} = p_T T\left(\frac{B^{n_T}}{B^{n_T} + {h_T}^{n_T}}\right)\left(\frac{1}{1 + ST_{ex}T_{ex}}\right) - K_{ex}\left(\frac{T^{n_{ex}}}{T^{n_{ex}} + h_{ex}^{n_{ex}}}\right)T - d_T\, T$$

$$\frac{dT_{ex}}{dt} = K_{ex}\left(\frac{T^{n_{ex}}}{T^{n_{ex}} + {h_{T_{ex}}}^{n_{ex}}}\right)T - d_{T_{ex}}T_{ex}$$

Table S3: T-B-Tex parameter estimates

T-B-Tex Model	Meaning	Units	Priors	Final Estimation
r_B	B cell growth rate	Day $^{-1}$	fixed	0.63
K_B	B cell carrying capacity	cells	fixed	0.24*10^6
a	Max killing rate of B cells by T cells	rate × cells^{-1}	[1,8]	3.75
n_B	Hill coefficient for T-mediated killing of B cells	dimensionless	fixed	1
h_B	Half-saturation for B cell killing	Cells/ml	[.005,.04] *10^6	0.032*10^6
n_T	Hill coefficient for T cell proliferation	dimensionless	fixed	1
h_T	Half-saturation for B-driven T cell proliferation	Cells/ml	[.0001-0.015] *10^6	0.001*10^6
p_T	T cell proliferation rate	Day $^{-1}$	[0.5-5]	1.87
d_T	T cell death rate	per day	[0.005-1.5]	0.011
k_{ex}	Exhausted T cell growth rate	Day $^{-1}$	[0.05-5]	0.17

n_{ex}	Hill coefficient for exhausted T cell proliferation	dimensionless	fixed	1
h_{ex}	Half-saturation for T cell driven proliferation	Cells/ml	[0.03-0.25]*10^6	0.006*10^6
dT_{ex}	Death rate of the exhausted T cell	Day $^{-1}$	[0.005-0.1]	0.12
sT_{exT}	suppression strength of Tex on T proliferation	Day $^{-1}$	[1e-7- 0.1]	8.15*10^{-8}

Hypothesis testing:

We tested two alternative TKI mechanisms by simulating the T–B–Tex model under two conditions: (1) H1, where TKIs act only on leukemic B cells by adding a constant 1.1/day B-cell killing term while keeping all T-cell parameters unchanged, and (2) H2, where TKIs both kill B cells and fully inhibit T-cell functions by setting $p_T = 0$, $d_T = 0$, and $K_{ex} = 0$. For each hypothesis, simulated T-cell trajectories were compared to experimental T-cell data using a Poisson log-likelihood, and a likelihood-ratio test determined which hypothesis better explained the observed T-cell behavior. We compared the simulated T-cell trajectories from each hypothesis to the experimental data using a Poisson log-likelihood and selected the model with the higher likelihood (Table S4). In both dasatinib- and ponatinib-treated conditions, H2 consistently achieved a dramatically higher likelihood than H1, leading to the selection of H2 as the mechanism best supported by the data

Table S4: Hypothesis testing using Poisson log-likelihood

Condition	LL(H1)	LL(H2)	Hypothesis Chose
Dasatinib + Blinatumomab	−8627.447	−424.705	H2
Ponatinib + Blinatumomab	−7407.142	−185.142	H2

Model Script:

Model T-B Folder:

i. TB model_fixed: ODE Function for Model T-B
ii. runMCMC_TB_fixed: MCMC function for Model T-B
iii. PriorFunction_fixed: Prior Function for Model T-B
iv. Loglikelihood_TB_fixed: Loglikelihood function for model T-B
v. Model1: main script

Model T-B-Tex Suppression Term Folder:

i. B_T_Tex_Model_v3: ODE Function for Model T-B-Tex
ii. runMCMC_v3: MCMC function for Model T-B-Tex
iii. loglikelihood_v3: Loglikelihood function for Model T-B-Tex
iv. PriorFunction_v3: Prior Function for Model T-B-Tex

v. runMCMC_v3

vi. newcode_Suppressionterm: main script

Hypothesis Testing Folder:

i. Test_drug_hypothesis: Hypothesis 1 and Hypothesis 2 testing

ii. Poisson_loglik: poisson likelihood function for calculating Loglikelihood

References

1. Liu C, Leighow SM, McIlroy K, et al. Excessive concentrations of kinase inhibitors in translational studies impede effective drug repurposing. Cell Rep Med 2023;4(10):101227.

2. Foucquier J, Guedj M. Analysis of drug combinations: current methodological landscape. Pharmacol Res Perspect;3(3):.

3. Roy V. Convergence diagnostics for markov chain monte carlo. Annu Rev Stat Appl 2020;7387–412.

4. Xing LEP. 16 : Approximate Inference : Markov Chain Monte Carlo Markov Chain Monte Carlo Concept of Markov Chain. 2017;1–9.

5. Nägele V, Zugmaier G, Goebeler ME, et al. Relationship of T- and B-cell kinetics to clinical response in patients with relapsed/refractory non-Hodgkin lymphoma treated with blinatumomab. Exp Hematol 2021;10032–36.

6. Dritschel H, Waters SL, Roller A, Byrne HM. A mathematical model of cytotoxic and helper T cell interactions in a tumour microenvironment. Lett Biomath 2018;5(sup1):S36–S68.

7. Hosseini I, Gadkar K, Stefanich E, et al. Mitigating the risk of cytokine release syndrome in a Phase I trial of CD20/CD3 bis pecific antibody mosunetuzumab in NHL: impact of translational system modeling. NPJ Syst Biol Appl;6(1):.

8. Sahoo P, Yang X, Abler D, et al. Mathematical deconvolution of CAR T-cell proliferation and exhaustion from real-time killing assay data. J R Soc Interface;17(162):.

Figure S1

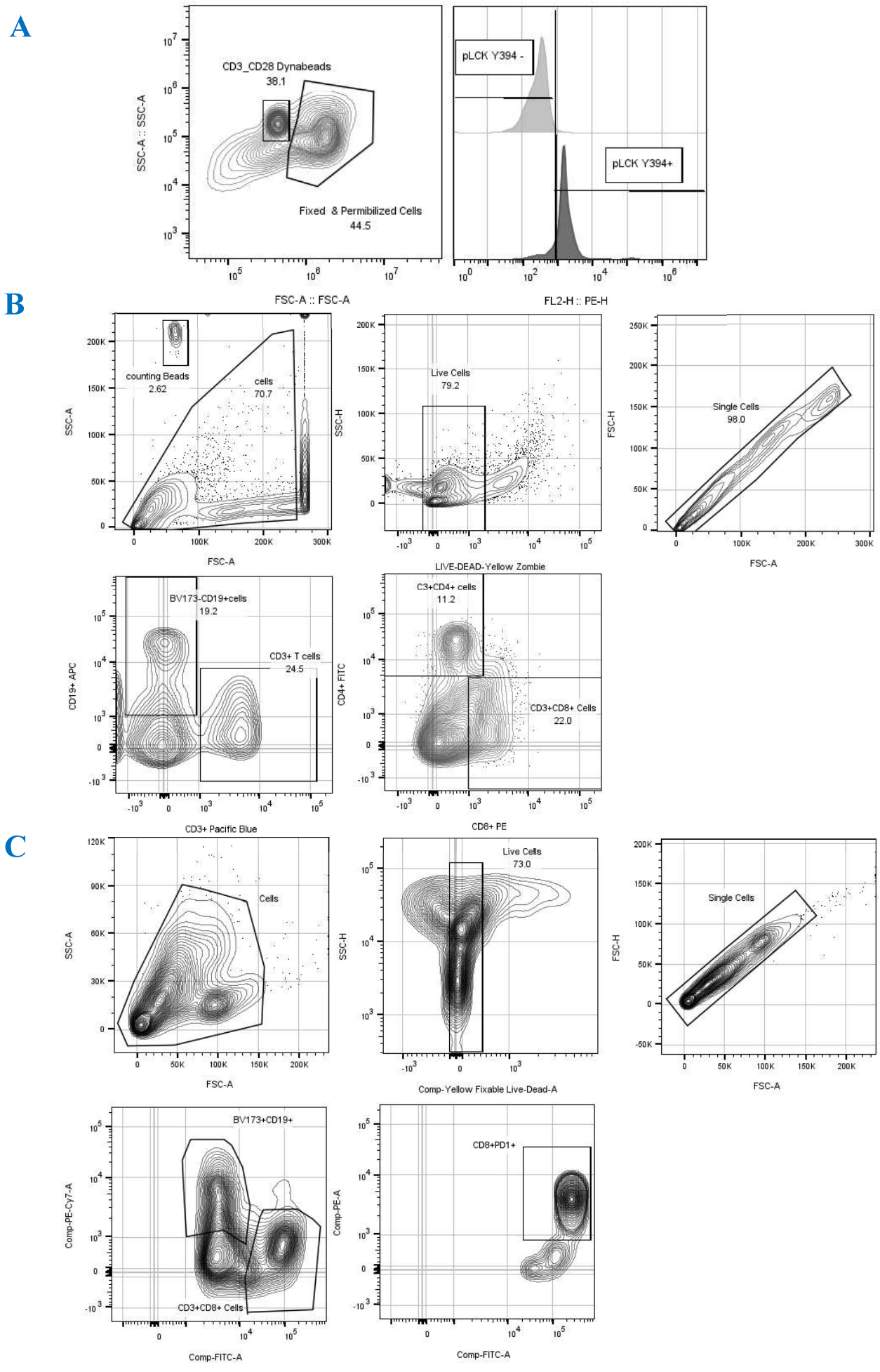
A
CD3_CD28 Dynabeads
38.1
Fixed & Permibilized Cells
44.5
SSC-A :: SSC-A
pLCK Y394 -
pLCK Y394+
B
FSC-A :: FSC-A
counting Beads
2.62
cells
70.7
SSC-A
FSC-A
SSC-H
FL2-H :: PE-H
Live Cells
79.2
FSC-H
Single Cells
98.0
FSC-A
BV173-CD19+cells
19.2
CD3+ T cells
24.5
CD19+ APC
CD3+ Pacific Blue
LIVE-DEAD-Yellow Zombie
C3+CD4+ cells
11.2
CD3+CD8+ Cells
22.0
CD4+ FITC
CD8+ PE
C
Cells
SSC-A
FSC-A
Live Cells
73.0
SSC-H
Comp-Yellow Fixable Live-Dead-A
Single Cells
FSC-H
FSC-A
BV173+CD19+
CD3+CD8+ Cells
Comp-PE-Cy7-A
Comp-FITC-A
CD8+PD1+
Comp-PE-A
Comp-FITC-A

Figure S1.* Gating strategy for Flow Cytometry Analysis. (A) Phospho-LCK analysis in Jurkat cells. Serum-starved cells were treated with TKIs for 2–4 hours, stimulated with CD3/CD28 Dynabeads (1:2), then fixed, permeabilized, and stained with a PE-conjugated antibody specific for pLCK Y394. $pLCK^+$ cells were quantified based on PE signal. (B) Co-culture analysis for combination treatments. Live cells were identified as Zombie Yellow–negative, and singlets were gated using FSC/SSC. Within singlets, T cells were gated as $CD3^+CD8^+$ and BV173 leukemia cells as $CD19^+$. (C) Gating for modeling-related experiments. Live Zombie Yellow–negative singlets were gated using FSC/SSC, followed by staining with CD8 and CD19. $CD8^+$ T cells were gated, and PD-1 expression was assessed within the $CD8^+$ population**.**

Figure S2

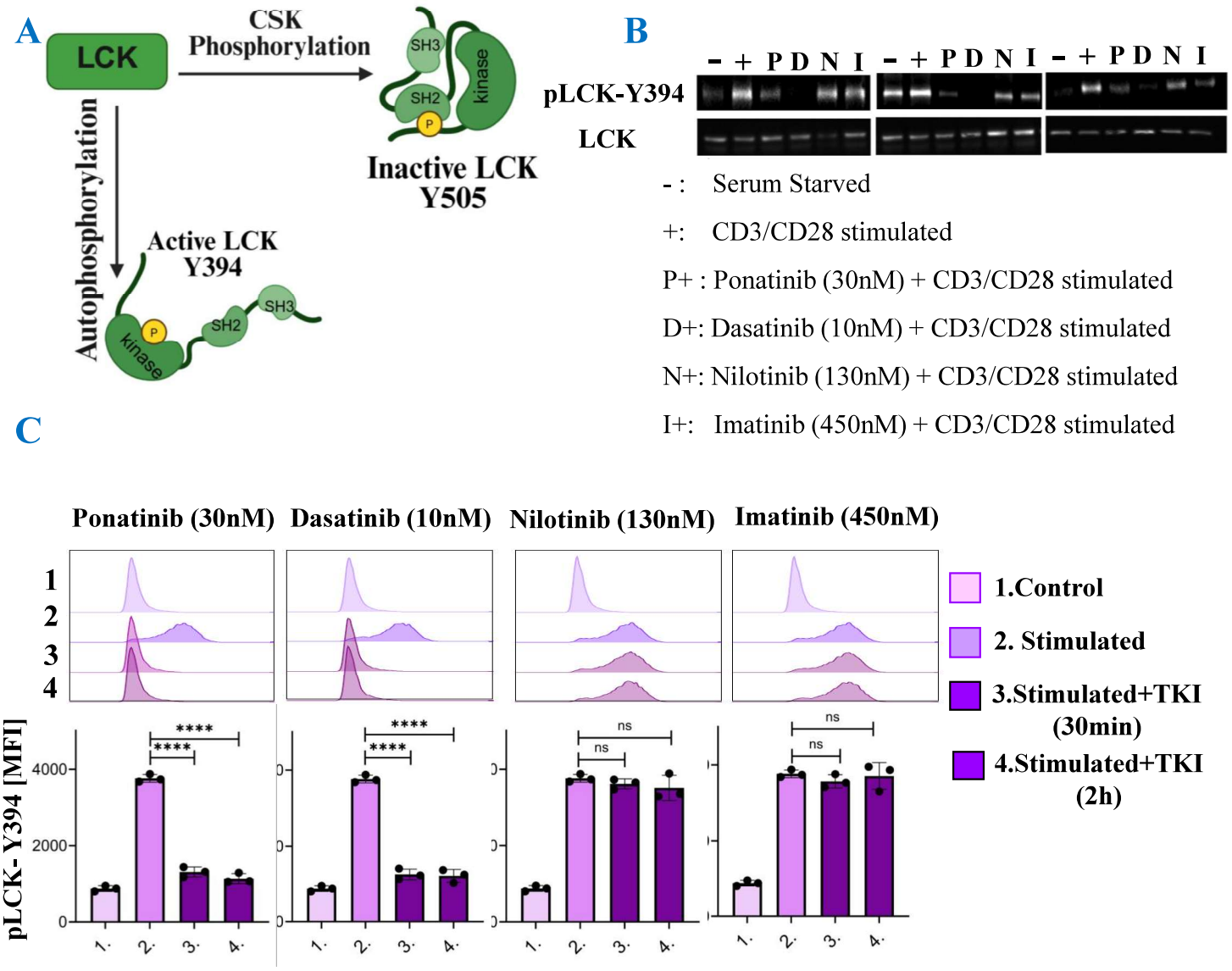

Figure S2. Rapid inhibition of LCK by Src tyrosine kinase inhibitors (TKIs). (A) Schematic illustrating regulation of LCK activity through phosphorylation of Y394 and Y505. Autophosphorylation at Y394 promotes TCR-proximal signaling, whereas CSK-mediated phosphorylation of Y505 inhibits LCK activity. (B) Western blot analysis of pLCK Y394 in serum-starved Jurkat cells treated with Src TKIs—ponatinib (P+), dasatinib (D+), nilotinib (N+), or imatinib (I+)—followed by CD3/CD28 stimulation. LCK Y394 levels were examined for 30 minutes, 2 hours, and 4 hours. (C) Flow-cytometric analysis of intracellular pLCK Y394 in Jurkat cells treated with TKIs at their clinically relevant concentrations for 2 hours and stimulated with CD3/CD28 for 30 minutes or 2 hours. Mean fluorescence intensity (MFI) values are shown for each condition.

Figure S3

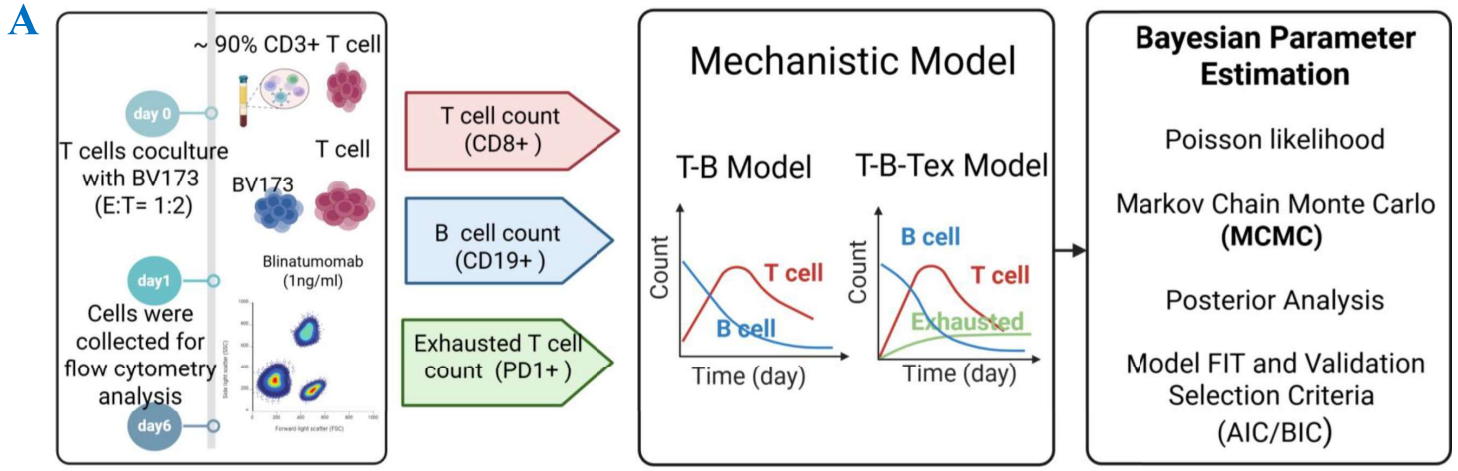

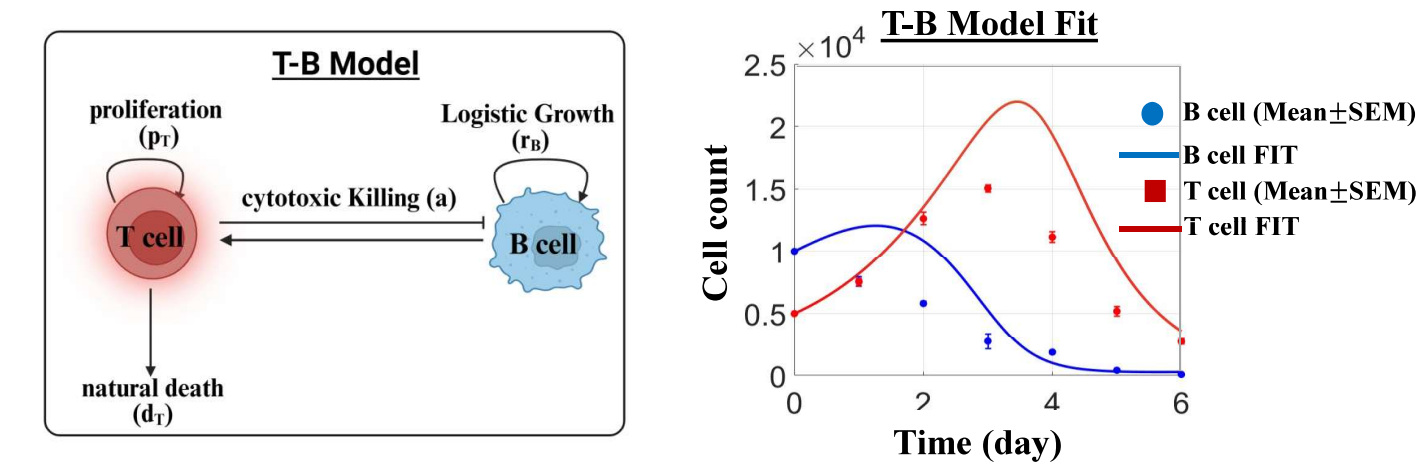

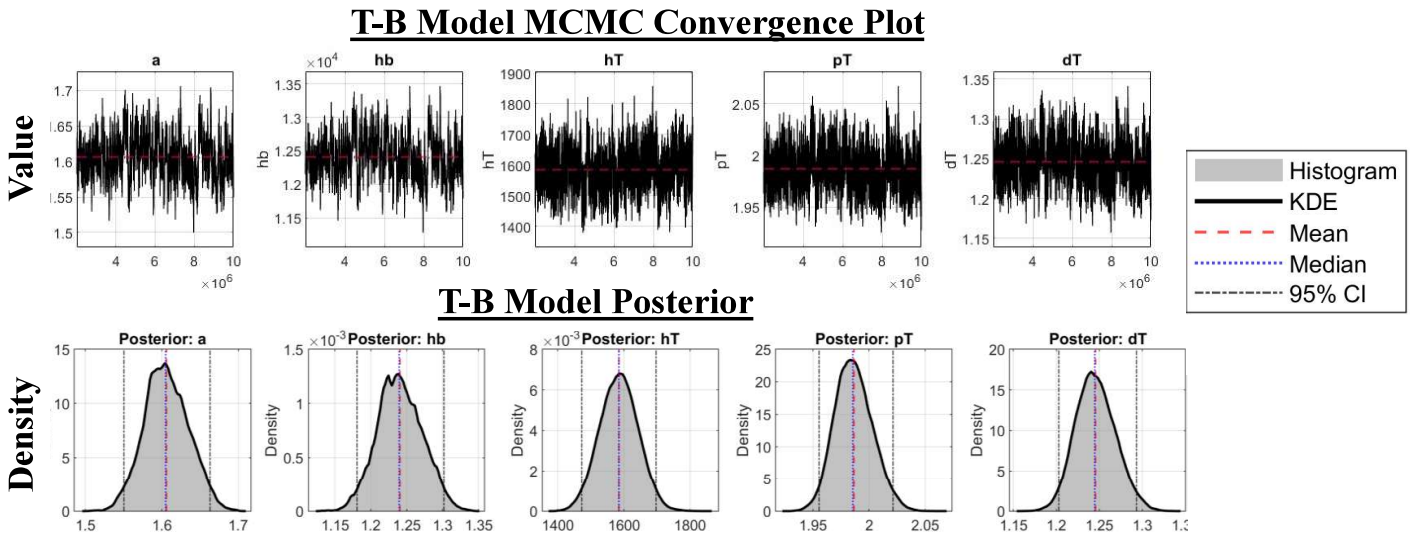

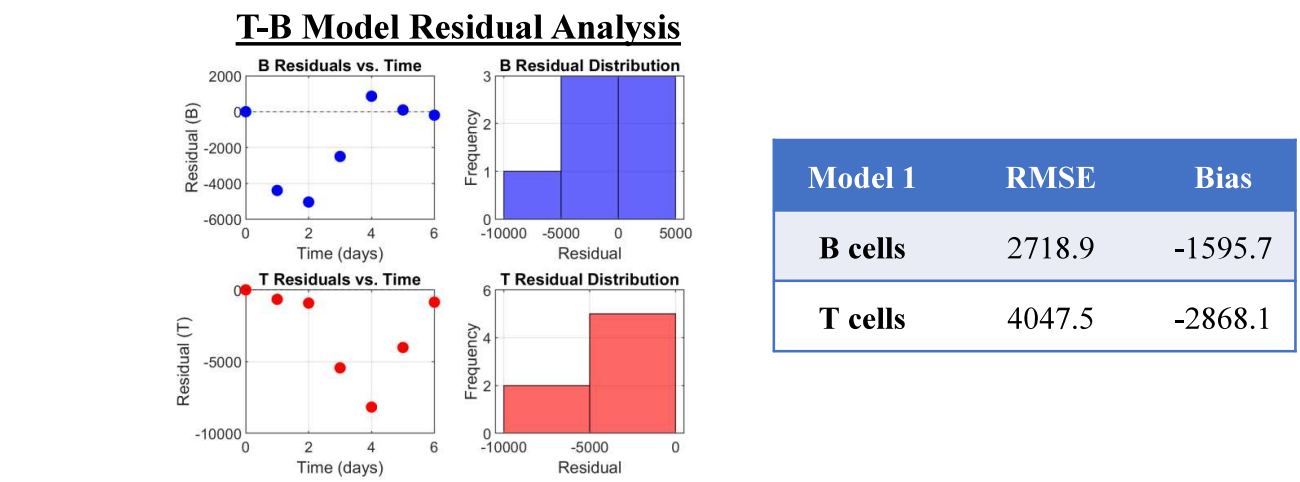

Model 1	RMSE	Bias
B cells	2718.9	-1595.7
T cells	4047.5	-2868.1

Figure S3:*Markov Chain Monte Carlo (MCMC) and residual analysis for model 1 parameter estimation. (A) Experimental setup for quantifying $CD19^+$ B cells, $CD8^+$ T cells, and $PD\text{-}1^+$ exhausted T cells in blinatumomab-treated co-cultures. Primary T cells and BV173 cells were plated at an effector-to-target ratio of 1:2 in round-bottom 96-well plates. Six independent replicates were analyzed daily for six days by flow cytometry. Gating strategy is shown in Supplementary Figure S1C. (B) Overview of the mathematical framework used for Model 1. An ordinary differential equation (ODE) model was constructed to describe temporal changes in B cells and T cells. Parameters were estimated using Markov Chain Monte Carlo (MCMC) fitting to experimental data. Model 1 includes logistic B-cell growth (rB, KB), T-cell-mediated B-cell killing (a, nB, hB), B-cell-dependent T-cell proliferation (pT, nT, hT), and natural T-cell death (dT). (C) MCMC results for Model 1 parameter estimation. Trace plots show mixing and convergence of sampled parameter values. Corresponding posterior distributions indicate parameter ranges and uncertainty. (D) Residual analysis comparing Model 1 predictions with experimental B-cell and T-cell counts over six days. Residuals are shown for all timepoints and both cell populations.

Figure S4

A

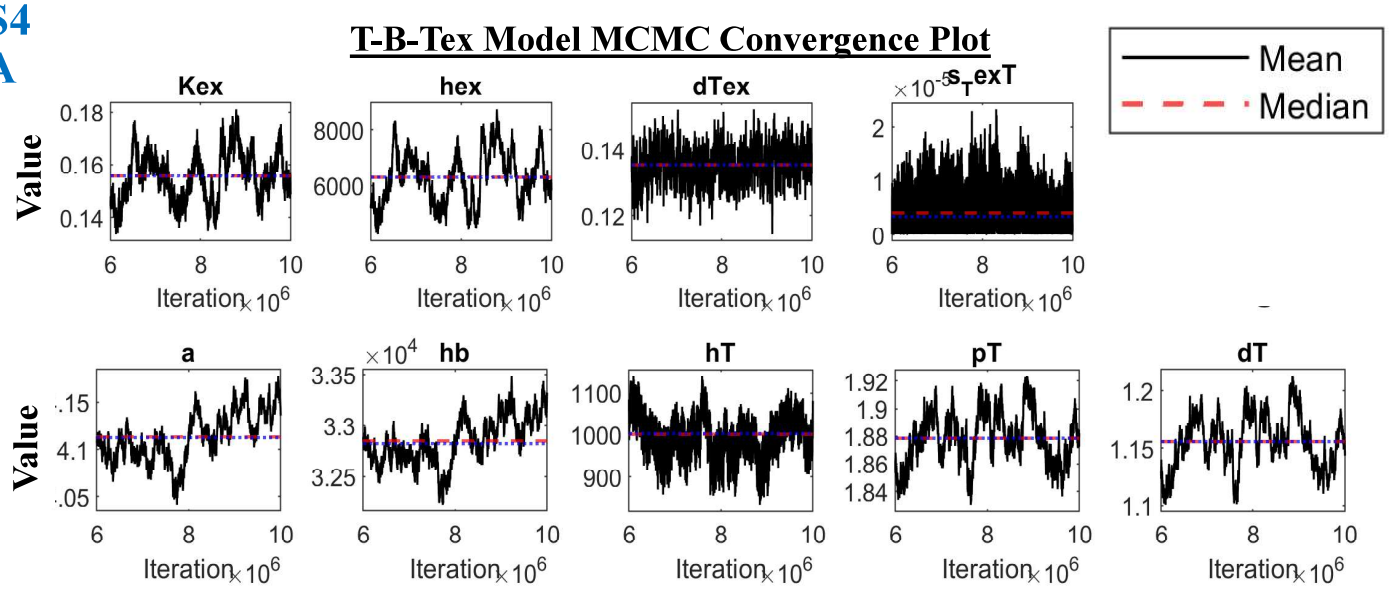

B

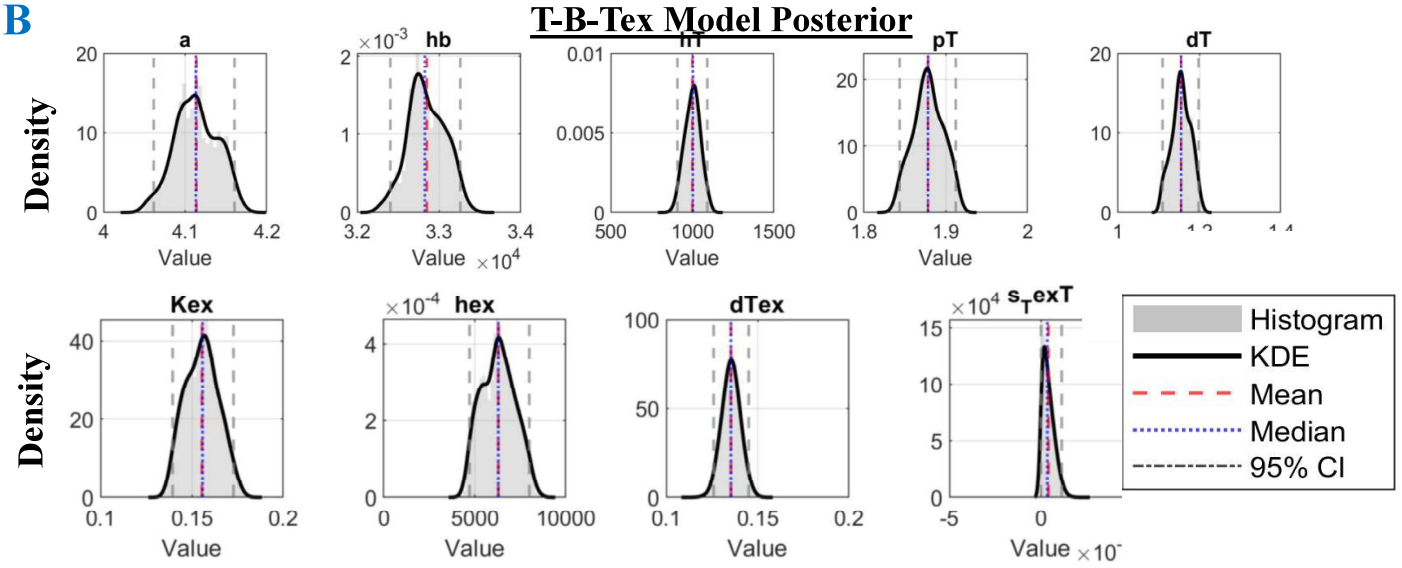

C

T-B-Tex Model Residual Analysis

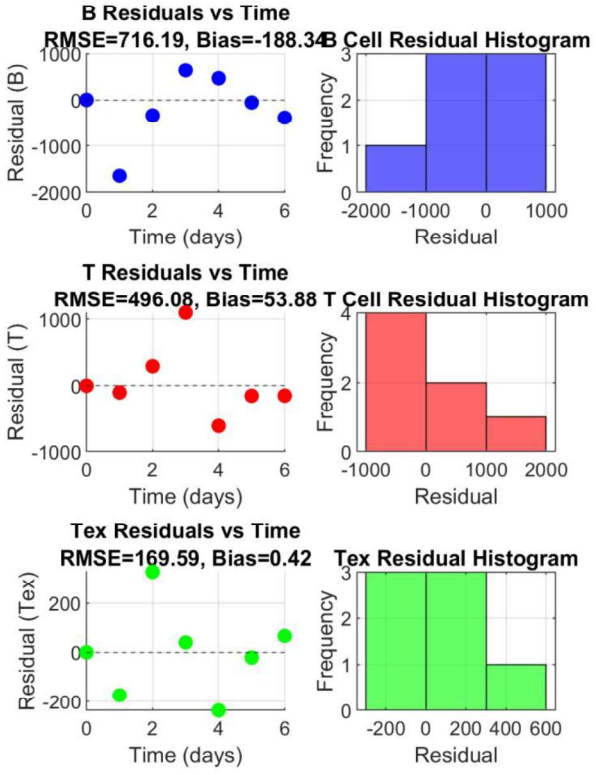

T-B-Tex Model	RMSE	Bias
B cells	716.19	-188.34
T cells	496.08	53.88
T_{ex} Cells	169.59	0.42

Figure S4:*Markov Chain Monte Carlo (MCMC) and residual analysis for model 2 parameter estimation. (A) Experimental setup for quantifying $CD19^+$ B cells, $CD8^+$ T cells, and $PD\text{-}1^+$ exhausted T cells in blinatumomab-treated co-cultures. Primary T cells and BV173 cells were plated at an effector-to-target ratio of 1:2 in round-bottom 96-well plates. Six independent replicates were monitored daily for six days by flow cytometry. Gating strategy is shown in Supplementary Figure S1C. (B) Overview of the mathematical modeling framework used to describe T–B dynamics. Model 1 incorporates logistic B-cell growth (r_B, K_B), T-cell-mediated B-cell killing (a, n_B, h_B), B-cell–dependent T-cell proliferation (p_T, n_T, h_T), and natural T-cell death (dT). Parameters were estimated by fitting the ODE model to experimental data using Markov Chain Monte Carlo (MCMC) methods. (C) MCMC parameter estimation results for Model 1. Trace plots show mixing and convergence of posterior samples. Posterior distributions are shown for all model parameters, illustrating parameter ranges and uncertainty. (D) Residual analysis for Model 1, comparing observed and simulated B-cell and T-cell counts over six days. Plots show residuals across all time points for both populations.

Figure S5

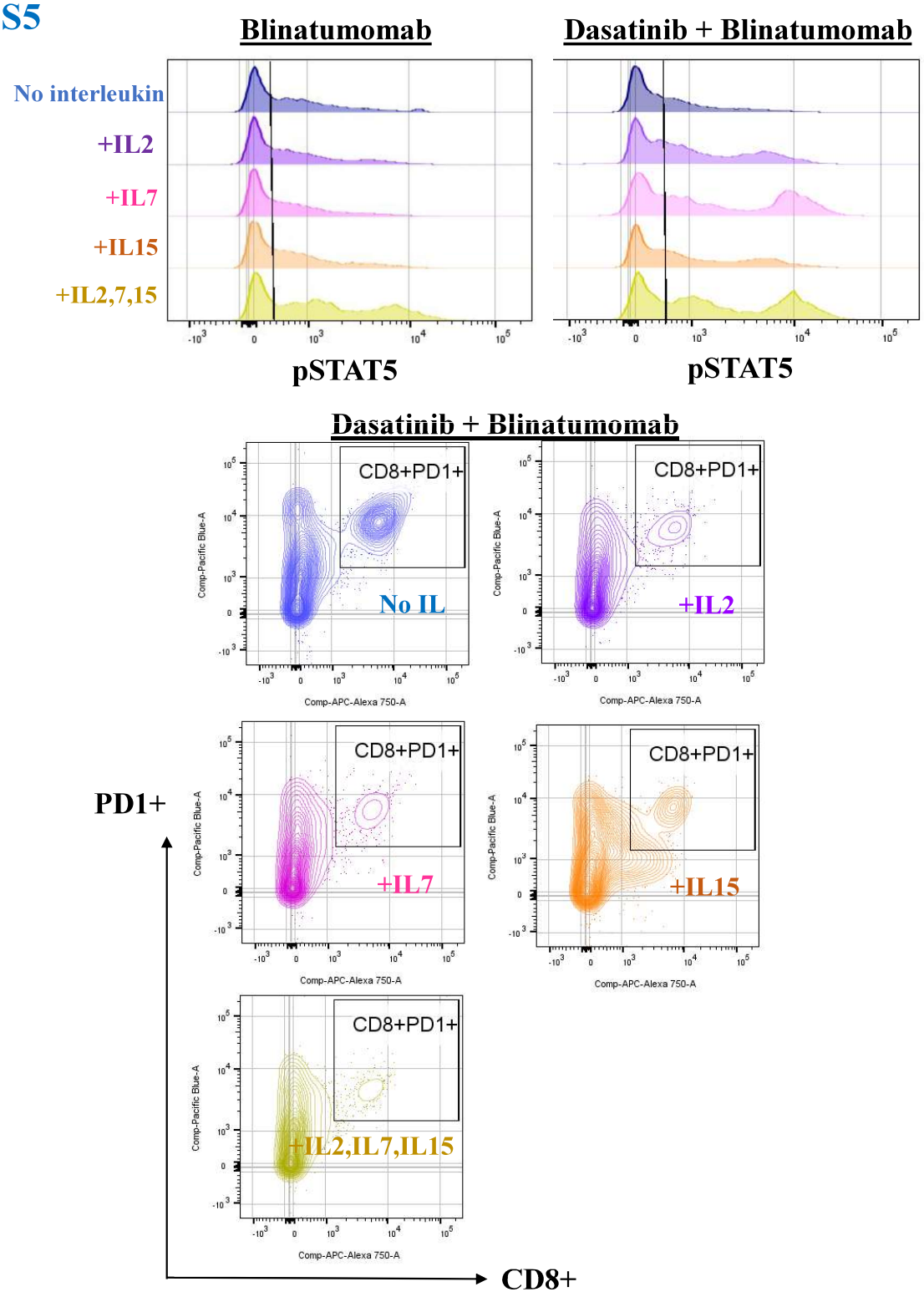

Figure S5:*Interleukins reverse the T cell exhaustion by Src/BCR-ABL TKIs through pstat5 signaling pathway. (A) Flow-cytometric analysis of intracellular pSTAT5 levels in T cells treated with blinatumomab alone or with interleukins (IL-2, IL-7, IL-15). Histograms show increased pSTAT5 following interleukin addition, both with blinatumomab alone and with blinatumomab plus dasatinib. (B) Gating of $CD8^+$ T cells and PD-1 expression for conditions shown in Figure 4. Flow plots show the percentage of $CD8^+$ $PD\text{-}1^+$ T-cells under dasatinib treatment, with interleukin addition partially reducing PD-1 expression.

Figure S6

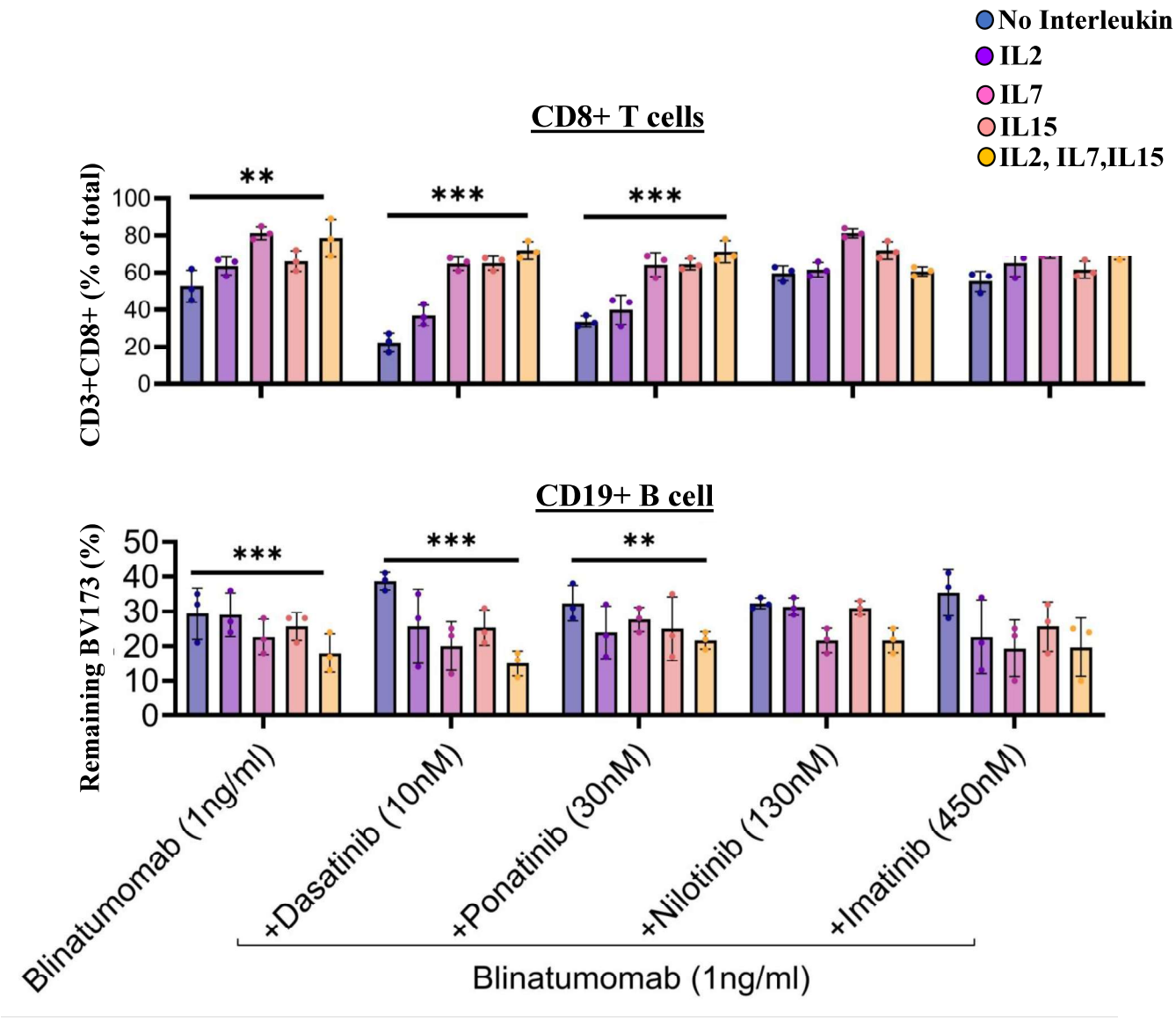

Figure S6:*Cytokines IL-2, IL-7, and IL-15 rescue the antagonistic effects of dual Src/BCR-ABL TKIs on Blinatumomab efficacy. Co-cultures of primary T cells and BV173 leukemia cells were treated for 48–72 hours with blinatumomab (1 ng/mL) alone or in combination with dual Src/BCR-ABL TKIs (dasatinib, ponatinib), BCR-ABL–selective TKIs (imatinib, nilotinib), and/or common γ-chain cytokines (IL-2, IL-7, IL-15; 10 ng/mL each). T-cell proliferation and BV173 cell clearance were quantified. Cytokine supplementation, particularly IL-7, restored T-cell expansion and enhanced blinatumomab-mediated leukemia cell killing in the presence of dual Src/BCR-ABL TKIs. Statistical significance was assessed using one-way ANOVA with Dunnett's post-hoc test comparing each treatment condition to blinatumomab alone. Significance thresholds: $P<0.05$ (*), $P<0.01$ (**), $P<0.001$ (***), $P<0.001$ (****), ns = not significant.